Harmonization of RBSP and ARASE energetic electron measurements utilizing ESA radiation monitor data

Ingmar Sandberg[1], Piers Jiggens[2], Hugh D. Evans[3], Constantinos Papadimitriou[1], Sigiava Aminalragia-Giamini[1], Christos Katsavrias[4], Alexander J. Boyd[5], Thomas Paul O'Brien[5], Nana Higashio[6], Takefumi Mitani[7], Iku Shinohara[8], Yoshizumi Mioshi[9], Daniel N. Baker[10], and Ioannis A. Daglis[11]

[1]Space Applications and Research Consultancy
[2]European Space Agency
[3]ESA
[4]University of Athens
[5]The Aerospace Corporation
[6]JAXA
[7]ISAS/JAXA
[8]Japan Aerospace Exploration Agency
[9]Nagoya University
[10]University of Colorado Boulder
[11]National and Kapodistrian University of Athens

November 23, 2022

Abstract

Accurate measurements of trapped energetic electron fluxes are of major importance for the studies of the complex nature of radiation belts and the characterization of space radiation environment. The harmonization of measurements between different instruments increase the accuracy of scientific studies and the reliability of data-driven models that treat the specification of space radiation environment. An inter-calibration analysis of the energetic electron flux measurements of the Magnetic Electron Ion Spectrometer (MagEIS) and the Relativistic Electron-Proton Telescope (REPT) instruments on-board the Radiation Belt Storm Probes (RBSP) versus the measurements of the Extremely High Energy Electron Experiment (XEP) unit on-board Arase (ERG) mission is presented. The performed analysis demonstrates a remarkable agreement between the majority of MagEIS and XEP measurements and suggests the re-scaling of MagEIS HIGH unit and of REPT measurements for the treatment of flux spectra discontinuities. The proposed adjustments were validated successfully using measurements from ESA Environmental Monitoring Unit (EMU) on-board GSAT0207 and the Standard Radiation Monitor (SREM) on-board INTEGRAL. The derived results lead to the harmonization of science-class experiments on-board RBSP (2012-2019) and Arase (2017-) and propose the use of the datasets as reference in a series of space weather and space radiation environment developments.

Harmonization of RBSP and ARASE energetic electron measurements utilizing ESA radiation monitor data

I. Sandberg[1], P. Jiggens[2], H. Evans[2], C. Papadimitriou[1], S. Aminalragia–Giamini[1], Ch. Katsavrias[1,3], A. J. Boyd[4], T. P. O'Brien[4], N. Higashio[5], T. Mitani[5], I. Shinohara[5], Y. Miyoshi[6],D. N. Baker[7],I. A. Daglis[3,8]

[1]Space Applications & Research Consultancy, Athens, Greece
[2]European Space Agency, European Research and Technology Centre, The Netherlands.
[3]Department of Physics, National and Kapodistrian University of Athens, Greece
[4]Aerospace Corporation, Chantilly, VA, USA
[5]Japan Aerospace Exploration Agency, Tsukuba, Japan
[6]Institute for Space-Earth Environmental Research, Nagoya University, Japan
[7]Laboratory for Atmospheric and Space Physics, Boulder, CO, USA
[8]Hellenic Space Center, Athens, Greece

Key Points:

- Cross-calibration analysis between Arase/XEP and RBSP/MagEIS & REPT measurements and validation using two different ESA radiation monitors
- Harmonization of science-class energetic electron flux measurements define reference dataset(s) for the outer Van Allen belt
- Reference datasets to be used for the harmonization of radiation monitors and the update/validation of climatological and space weather models.

Corresponding author: Ingmar Sandberg, `sandberg@sparc.gr`

Abstract

Accurate measurements of trapped energetic electron fluxes are of major importance for the studies of the complex nature of radiation belts and the characterization of space radiation environment. The harmonization of measurements between different instruments increase the accuracy of scientific studies and the reliability of data-driven models that treat the specification of space radiation environment. An inter-calibration analysis of the energetic electron flux measurements of the Magnetic Electron Ion Spectrometer (MagEIS) and the Relativistic Electron-Proton Telescope (REPT) instruments on-board the Radiation Belt Storm Probes (RBSP) versus the measurements of the Extremely High Energy Electron Experiment (XEP) unit on-board Arase (ERG) mission is presented. The performed analysis demonstrates a remarkable agreement between the majority of MagEIS and XEP measurements and suggests the re-scaling of MagEIS HIGH unit and of REPT measurements for the treatment of flux spectra discontinuities. The proposed adjustments were validated successfully using measurements from ESA Environmental Monitoring Unit (EMU) on-board GSAT0207 and the Standard Radiation Monitor (SREM) on-board INTEGRAL. The derived results lead to the harmonization of science-class experiments on-board RBSP (2012-2019) and Arase (2017-) and propose the use of the datasets as reference in a series of space weather and space radiation environment developments.

Plain Language Summary

Accurate measurements of trapped energetic electron fluxes are of major importance for the studies of the complex nature of radiation belts and the characterization of space radiation environment. The harmonization of measurements between different instruments increase the accuracy of scientific studies and the reliability of data-driven models that treat the specification of space radiation environment. This work lead to the harmonisation of the relativistic electron flux datasets from the cornerstone US and Japanese Radiation Belt missions. The derived results are validated by European Space Agency radiation monitors and can be used in a series of applications and developments.

1 Introduction

The dynamics of the Earth's magnetosphere provides an efficient mechanism for the trapping and the acceleration of energetic particles. At the Earth's magnetic equator, the outer belt extends from an altitude of just over 10,000 km to distances beyond geostationary orbit and is dominated by trapped electrons. The electron peak flux is energy-dependent but is typically at an orbit altitude between 3.5 and 5 Earth radii at the magnetic equatorial plane. The relativistic electron population in the outer Van Allen radiation belt is extremely variable — especially during periods of enhanced geomagnetic activity - as it is subjected to processes, such as loss and acceleration, which compete and can deplete or enhance electron populations (Turner et al., 2015; Reeves et al., 2016). For satellites, the outer belt poses a significant hazard since the intense electron fluxes cause ionizing dose, non-ionizing energy loss and internal charging. For the better understanding of the physical mechanisms associated with the dynamics of the outer belt it is critical to have accurate flux measurements of the trapped energetic electrons. This case is usually met in the high energy resolution measurements of detectors that constitute part of scientific experiments. Such datasets are usually considered as reference for the in-flight evaluation and calibration of radiation monitors on-board other satellites. The use of cross-calibrated measurements - under a common reference - can be vital for the derivation of coherent model outputs from data-driven engineering models that treat the characterization of the space radiation environment, e.g. (O'Brien et al., 2018). One such example is the Solar Energetic

Particle Environment Modelling reference dataset (SEPEM RDS) (Heynderickx et al., 2018), based on NOAA GOES proton flux measurements (Onsager et al., 1996), cross-calibrated by Sandberg et al. (2014) using as reference the IMP-8 Goddard Medium Energy experiment (Richardson et al., 2008). SEPEM RDS has resulted to the production of spectrally coherent outputs in various solar energetic proton environment models (Jiggens et al., 2018; Aminalragia-Giamini et al., 2018). For the case of the trapped radiation environment, cornerstone missions that carry science-class electron detectors - after the CRRES era (1990-1991) (Johnson & Kierein, 1992) - are the Radiation Belts Storm Probes (RBSP) (Mauk et al., 2012) and more recently the Exploration of energization and Radiation in Geospace Arase (ERG) (Miyoshi et al., 2018a). The RBSP are twin spin–stabilized spacecraft assigned with the study of the radiation belts and the inner magnetosphere. The probes were launched on August 2012 in near–equatorial highly elliptic orbit (HEO) with 10.2° inclination and a period of ∼ 9 hours (perigee at 618 km and apogee about 30,000). RBSP-B was deactivated on July 2019 and RBSP-A three months later. The electron data analysis from the science class detectors MagEIS (Blake et al., 2013) and REPT (Baker et al., 2012) on-board RBSP led to a series of investigations and breakthrough discoveries, e.g (Baker et al., 2014; Mann et al., 2016) related to the electron belt dynamics and the physical mechanisms responsible for electron losses and energization. The Arase mission is a newer science mission, developed by JAXA in collaboration with universities and institutes in Japan and Taiwan, aiming to study electron acceleration and loss mechanisms in the outer radiation belt. The mission was launched on December 2016 and initiated its scientific observations three months later in elliptic orbit with 31° inclination and a period of ∼ 8 (perigee at 400 km and apogee at 32,000 km). Arase carries, among others, the extremely high-energy electron experiment (XEP) (Higashio et al., 2018a) which provides electron flux measurements at energies above 0.3 MeV.

In this work, we have performed and validated successfully an inter-calibration of the electron flux measurements of MagEIS and REPT versus those of XEP - utilising measurements from two ESA radiation monitors. The resulting harmonized datasets can be considered as reference for use in a series of application and models; for the calibration of space radiation detectors on-board satellites the orbits of which cross the HEO of RBSP and Arase, for the building/evaluation of quantitative climatological/engineering models, and for the development/validation of radiation belt forecasting space weather models. Section 2 presents the characteristics of the datasets considered and Section 3 presents the derivation of the harmonization factors accounting for RBSP datasets. In Section 4, a validation study is presented using the deep charging current measurements of the Environmental Monitoring Unit (EMU) (Sandberg et al., 2019) on-board Galileo satellite GSAT207 and the measurements from Standard Radiation Monitor (SREM) (Mohammadzadeh et al., 2003) on-board INTEGRAL (Evans et al., 2008).

2 RBSP and ARASE electron flux measurements

MagEIS and REPT instruments are part of the Energetic Particle Composition and Thermal Suite (ECT). MagEIS utilizes a strong magnet to steer electrons into a set of solid state detectors (SSD), providing flux measurements of ∼ 30 keV to 4 MeV (Blake et al., 2013). MagEIS consists of four units: the LOW measures low-energy electrons (∼30–200 keV), two MEDIUM units measure electrons of ∼200 keV to 1 MeV and the HIGH measures relativistic electrons (∼1–4 MeV). We have used the background-corrected Level-2 Release-4 spin-averaged flux MagEIS datasets (Claudepierre et al., 2015). The energy values assigned to MagEIS channels in this study, correspond to the mean values of the twin units (Table 1) accounting from 03-08-2013. For the derivation of the cross-calibration factors, we use measurements

with background correction error (FESA_ERROR) above 50% similar to Boyd et al. (2019).

REPT uses a stack of SSD and provides relativistic electrons measurements in 10 channels, the energy efficiency of which is characterized by long "tails" (Baker et al., 2012). The derivation of the REPT electron differential fluxes - within 1.9 - 12.3 MeV - was performed using the bow-tie analysis method, e.g. Van Allen et al. (1974). The present study demonstrates results for the channels up to 9.3 MeV (Table 1). We have analyzed the Level-2 Release-3 datasets which include background measurements induced by the galactic cosmic rays. For the subset of measurements that overlap Arase ones, the background level was estimated for each channel - using a cut-off threshold as it did not present significant modulations - and subtracted. For the needs of the harmonization studies, a 3-minutes time-averaged ECT dataset was created to match the resolution of XEP measurements.

XEP unit (Higashio et al., 2018a) includes a detection system that contains five SSD that measure electrons in the energy range of $0.4 - 5.4$ MeV. The first SSD is 50 μm thick, while the others are 1500 μm thick. An aluminum shield (130 μm thick) is placed in front of the first SSD to prevent the intrusion of light and electrons with $E < 0.4$ MeV. The present study is based on the use of Level-2 version 01-00 electron omni-directional fluxes binned in nine energy channels - within a time period from 20-03-2017 until 31-8-2019. The measurements of each channel were assigned to the geometric mean of its energy bin boundaries $E_{XEP} = (0.55, 0.69, 0.89, 1.09, 1.34, 1.64, 1.98, 2.48, 3.13)$ MeV.

3 Harmonization of ECT and XEP datasets

The comparisons between ECT and XEP electron measurements are based on the determination of suitable conjunctions between the orbits of the carrier satellites. The conjunctions may be defined as the spatio-temporal positions where the detectors are expected to encounter the same population of trapped electrons. The search criteria for obtaining these positions were defined on the basis of the adiabatic invariants of electron motion. We have followed the spirit of the recommendations of the Panel on Radiation Belt Environment Modeling (S. Bourdarie et al., 2008) but required stricter criteria for the spatiotemporal conditions, namely $\delta L \leq 0.01$, $\delta(\alpha_{eq}) \leq 2$, $\delta t \leq 1$ hour, $\delta(MLT) \leq 12$ hours. Here, L denotes the L-shell value, α_{Eq} the equatorial pitch angle and MLT the magnetic local time. The magnetic coordinates were derived using the UNILIB library (Heynderickx et al., 2000) assuming the IGRF model for the internal, and the quiet Olson-Pfitzer 1977 (Olson & Pfitzer, 1977) model for the external magnetic field components. The application of these criteria resulted to 2853 magnetic conjunctions within $4.3 \leq L \leq 6.5$; the criterion for using conjuctions during quiet magnetospheric conditions, i.e. $K_p < 2$ for the last 2 days - defined from now on as the "quiet" conjunctions - was adopted only for the calibration of the $E < 3.0$ MeV ECT channels. For the flux comparisons we re-binned XEP fluxes to the ECT energies. For the values within the XEP energy range a piece-wise power-law interpolation was applied and for extrapolating the values below (or above), a performed non–linear least square fitting was performed using the first (or last) three points of each XEP flux spectrum. As a fit function we used an exponential cut-off power-law. This procedure allowed us to perform quantitative comparisons between the re-binned XEP f_{XEP} and the ECT energetic fluxes f_{ECT}. In Figure 1, we present box-and-whisker plots of the flux ratios (f_{ECT}/f_{XEP}). The yellow boxes correspond to the available spatiotemporal conjunctions and the blue ones to the "quiet" conjunctions. The box-and-whiskers for the MagEIS comparisons (upper plot) indicate a remarkable agreement between the calibration of XEP and MEDIUM channels ($E < 1$ MeV) which becomes evident when the quiet magnetospheric conditions are considered (i.e. blue boxes). For $1.06 \leq E \leq 2.59$ MeV, MagEIS/HIGH and XEP channels differ by a factor less than two

Table 1. Scaling factors for the harmonization of ECT to XEP electron fluxes.

MagEIS energy channels

E[MeV]	median	$sf\,\vert\min(MSE)$	conjunctions
0.176	1.03	1.04	140
0.240	0.97	0.88	406
0.350	0.98	0.90	405
0.470	0.99	0.94	370
0.600	0.94	0.93	307
0.749	0.94	0.91	294
0.904	0.87	0.86	190
1.064	1.35	1.30	215
1.575	1.37	1.38	262
1.728	1.23	1.22	259
2.254	1.23	1.27	87
2.589	1.51	1.72	62
3.536	0.84	0.73	73
3.970	1.79	1.71	58

REPT energy channels

E[MeV]	median	$sf\,\vert\min(MSE)$	conjunctions
1.9	4.52	3.87	422
2.1	2.22	2.20	369
2.6	1.80	2.00	251
3.4	2.21	1.97	652
4.2	1.91	1.65	400
5.2	2.37	2.31	322
6.3	1.45	1.43	91
7.7	0.29	0.24	12
9.9	1.07	1.07	1

while the differences between yellow and blue box-and-whiskers are not significant. The differences which appear for the last two HIGH channels, for $E > 3.5$ MeV, are attributed to the drastic decrease of the available ultra-relativistic electron flux measurements during quiet conjunctions. The box-and-whisker plot accounting for the REPT comparisons (lower plot) reveals a consistent difference with XEP - of the order of two - for the energies at $2.1 \leq E \leq 6.3$ MeV, while the deviation at 1.9 MeV is larger. For $E \leq 6.3$ MeV, the differences between blue and yellow box-and-whiskers are not significant. For the channels above 6.5 MeV, however, measurements of ultra-relativistic electrons appear only during active magnetospheric conditions. In view of the above, we consider the use of the "quiet" conjunctions only for the derivation of the scaling factors for the ECT channels below 3.0 MeV. The scaling factors, may be defined either as the median values of the ratios (f_{ECT}/f_{XEP}), or as the factors that minimize the mean squared error (MSE) between f_{XEP} and f_{ECT} series, defined here as $sf\,\vert\min(MSE)$. Table 1 lists these values, together with the number of the available conjunction measurements used for each energy channel.
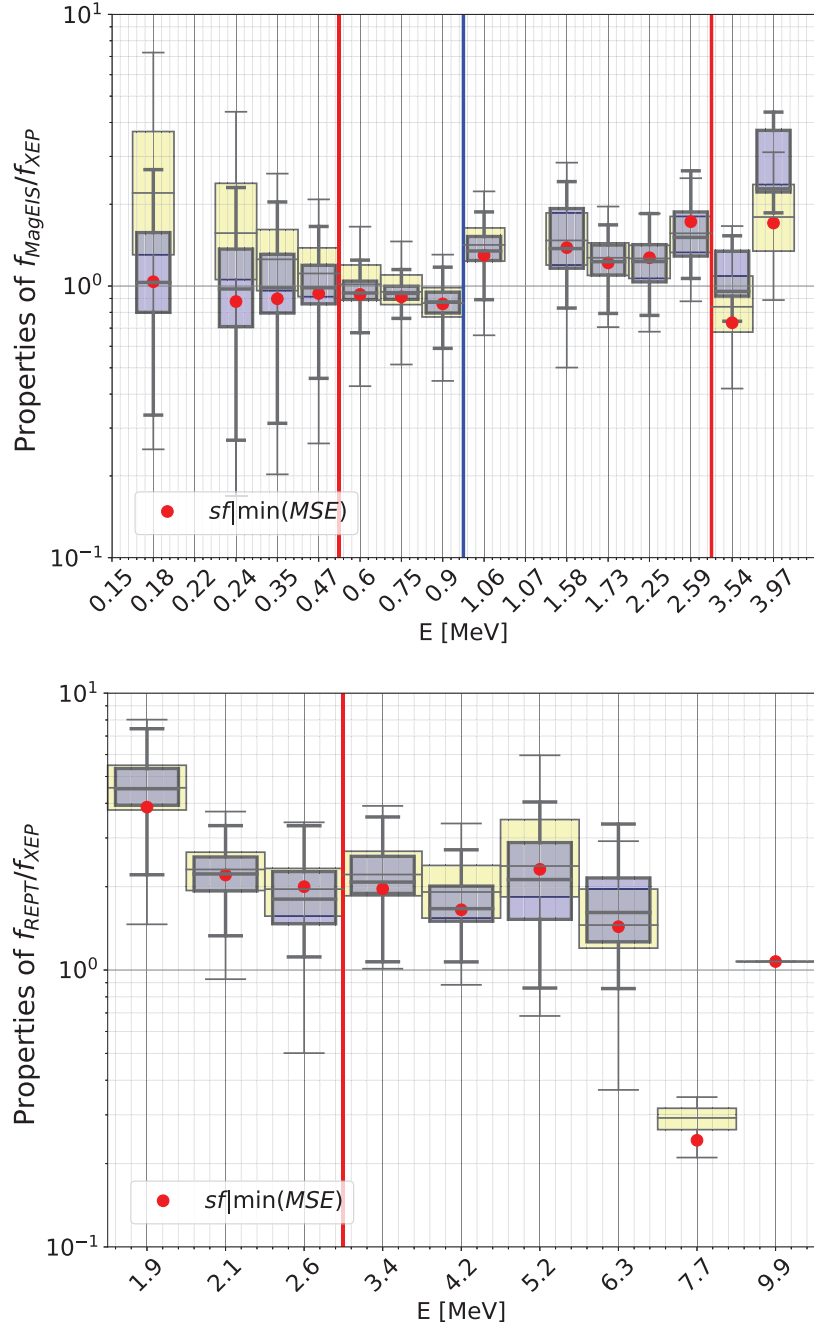
Figure 1. Box-and-whiskers for the ratios f_{MagEIS}/f_{XEP} (upper plot) and f_{REPT}/f_{XEP} (lower plot). The yellow boxes include the measurements during the spatiotemporal conjunctions and the blue boxes - with the thick whiskers - to "quiet" conjunctions. The blue line perpendicular to the energy axis separates the MEDIUM and the HIGH channels. The red line(s) define the ECT channels that fall within the XEP energy range. The red circles denote the values that - when divide the ECT fluxes - achieve an MSE minimization with the re-binned XEP fluxes when all (quiet) conjunctions are considered for $E > 3$ ($E < 3$) MeV.

Figure 2 presents - as example - cross-plots between the re-scaled ECT f_{ECT}/sf and the re-binned f_{XEP} fluxes for the 0.47 MeV MagEIS and the 6.3 MeV REPT channels. The ECT adjustments have been performed by dividing either by the *median* or by the $sf|min(MSE)$ values (cf. Table 1). Note that points which were not taken into account in the calculation of the adjustment factors - i.e. measurements with large statistical error or within the background - are included in these plots.
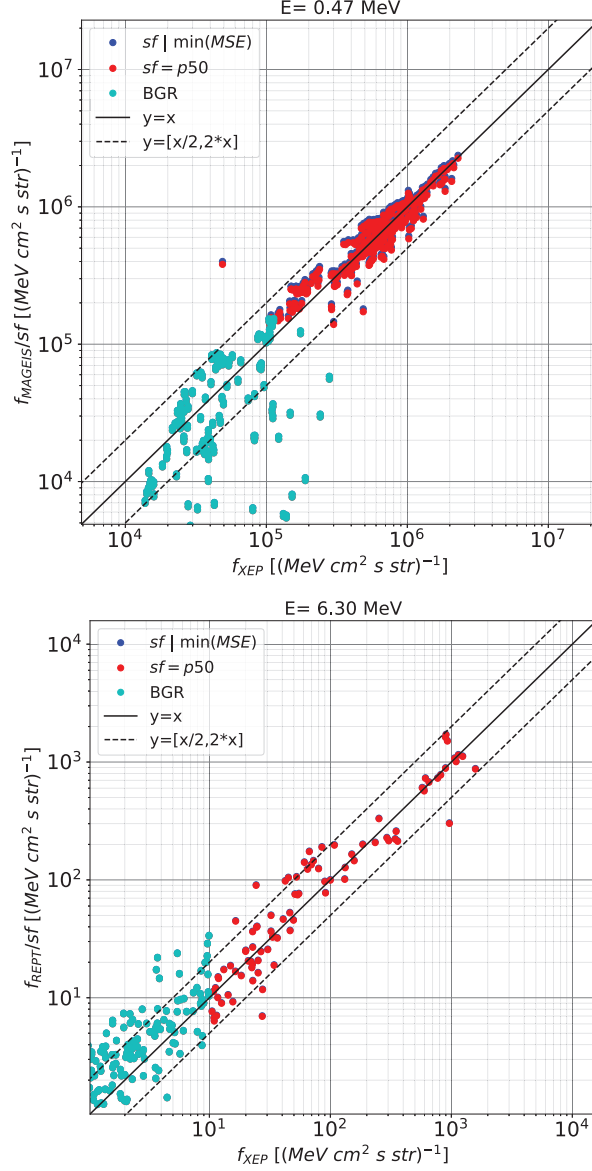
Figure 2. Cross plots between the re-scaled MagEIS (REPT) electron differential fluxes versus the interpolated XEP fluxes re-binned at 0.47 MeV (6.30 MeV) using the quiet (all the) spatio-temporal conjunctions. The red circles correspond to the ECT fluxes divided by the median value (P50) and the blue by the factor $sf|min(MSE)$. The ciel circles denote measurements which were not considered in the derivation of the scaling factors.

The derived results demonstrates a remarkable agreement between MEDIUM and XEP measurements and suggests the re-scaling of HIGH and REPT measurements. The proposed adjustments, as listed in Table 1 lead to the harmonization of the science-class high energy experiments on-board RBSP (2012-2019) with Arase (2017-). The differences between the re-scaling factors for MagEIS/MEDIUM, MagEIS/HIGH and REPT units can be attributed to the different calibration procedures applied separately for each unit and to the increased background of the last HIGH channel. The performed studies indicate also the necessity for relaxing the K_p - related restrictions (S. Bourdarie et al., 2008) for the cross-calibration of relativistic electron flux measurements; during quiet magnetospheric conditions the measured fluxes are typically of low intensity and below the instrument's background levels. Last, but not least it should be noted that REPT team has recently found a missing factor of two in the data processing software. Next data releases will address this issue (communication with Shri Kanekal, NASA) resulting to an improved agreement with XEP.

4 Validation of data harmonization

4.1 ESA radiation monitors

For the validation of the ECT adjustments suggested by XEP comparisons, we utilized measurements from ESA radiation monitors on-board missions the orbits of which cross the near equatorial HEO of RBSP. Such conditions are met by the EMU on-board Galileo satellites and the ESA SREM on-board INTEGRAL mission. Both of these sensors have been calibrated by means of GEANT4 simulations (Agostinelli et al., 2003) and provide healthy measurements. The EMU is a radiation sensitive instrument designed for use in the orbit of the GNSS Galileo constellation. Two units are currently flying; the first one is on-board GSAT0207, launched on November 2016, while the second unit is on board GSAT0215 launched on December 2017. EMU includes a SURF sensor (Ryden et al., 2015), composed of a stack of eight charge collecting plates which measure internal charging currents. The unit is mounted on the spacecraft panel with a view in the East-West direction, e.g. $\sim 90°$ pitch angle. SURF data have been used for the creation of differential electron flux dataset within $0.2 - 8.0$ MeV by Sandberg et al. (2019). Here, we use the primary internal charging current measurements from the last four GSAT0207/EMU/SURF plates utilizing the response function derived by modeling the shielding impact of the host spacecraft by a Ta slab of 5 cm thickness. SREM unit consists of three SSD in a two-detectors-head configuration and measures electrons with $E > 0.5$ MeV and protons with $E > 10$ MeV. SREM samples electron fluxes in rather broad and overlapping energy bands providing measurements in 15 channels. The units on-board STRV-1C, Rosetta, GIOVE-B, Herschel and Planck spacecraft have completed their operation while those on-board Proba-1 and INTEGRAL continue to provide healthy measurements after two decades. Here we use the count-rate measurements from the INTEGRAL/SREM $S12$, $S13$ and $C4$ channels utilizing their electron response functions for the derivation of which a mass model that included the host spacecraft was used. SREM is typically directed along a pitch angle of $\sim 90°$. Figure 3 presents the electron response functions of the channels selected from both ESA radiation monitors.
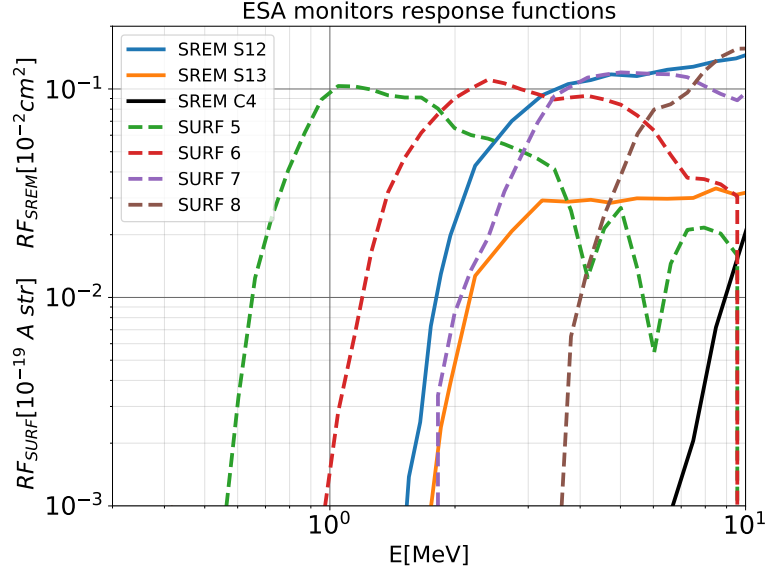
Figure 3. Electron response functions of INTEGRAL/SREM and GSAT0207/EMU selected channels.

₂₃₈ **4.2 Validation approach and results**

₂₃₉   The validation approach considered is to compare ECT and ESA radiation mon-
₂₄₀ itor measurements before and after the application of the XEP-induced scaling factors
₂₄₁ $sf|min(MSE)$. The spatiotemporal conjunctions were determined using the same cri-
₂₄₂ teria presented in Section 3; 1830 RBSP conjunctions were found with GSAT0205 and
₂₄₃ 830 with INTEGRAL.
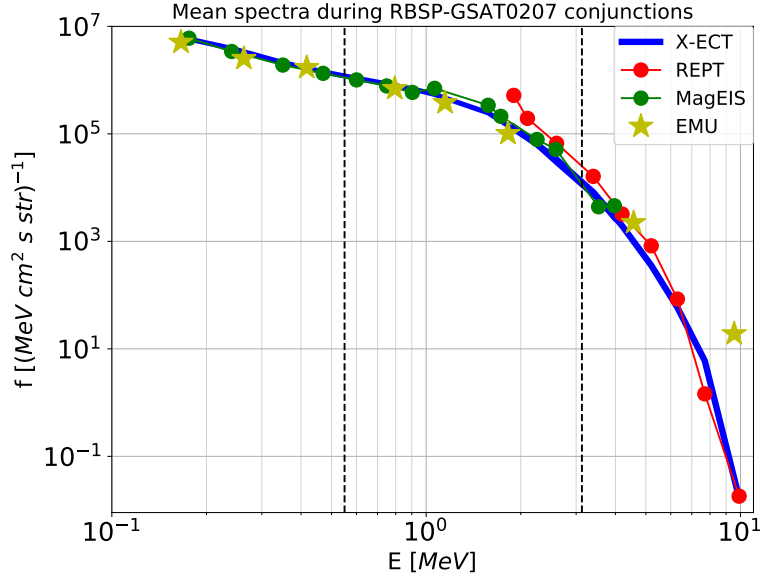
Figure 4. RBSP/ECT mean flux spectra during the conjunctions with GSAT0207. The re-scaled spectrum (blue line) is presented versus the original MagEIS (green circles) and REPT (red circles) spectra. The mean flux spectrum of GSAT0207/EMU is also presented (gold stars).

Figure 4 presents the mean electron flux spectra of ECT and EMU for the RBSP-GSAT207 conjunctions. It is evident that the re-scaling of ECT data treat the mismatches between MagEIS/MEDIUM, MagEIS/LOW and REPT calibrations leading to a coherent spectra over 4 orders of magnitude. We note that these adjustments may be particularly important in phase space density calculations which are sensitive on the flux spectrum slope. It's worth-mentioning that the adjusted ECT spectrum seems to exhibit 2 breaks at ~ 0.3 and ~ 1.8 MeV which is consistent with the three-step scenario (Jaynes et al., 2015; Katsavrias et al., 2019) to describe the different acceleration mechanisms from seed (100 - 300 keV), to relativistic (up to 2 MeV) and ultra-relativistic (>2 MeV) electrons. The bow-tie derived EMU spectra is found to be in very good agreement, up to 5 MeV, in accordance to Sandberg et al. (2019). It remains still the question if the proposed adjustments lead to improvements in terms of the absolute flux values per se. In order to confirm that, we fold the ECT fluxes $f(E)$ with the response function RF_i of each monitors' channel i;

$$C_{rec,i} = \int_0^{E_{max}} f(E)RF_i(E)dE, \tag{1}$$

and calculate the reconstructed measurements $C_{rec,i}$. The latter ones were compared with the actual measurements C_i using the median values of their ratios $M(i) = median(C_{rec,i}/C_i)$. For the case of SURF plates, MagEIS and REPT spectra were merged to construct $f(E)$, while for SREM, only the REPT spectra were considered. The same procedure was repeated for the calculation of the median values $M'(i)$ derived using the re-scaled ECT fluxes. The modification in the median values accounting for the reconstructed measurements are presented in Table 2; the median values for SURF plates $5-8$, reached values closer to one after the re-scaling. The same trend was also observed for the case of SREM channels as well. In support to the above, we calculated for each channel the energy integration limit E_{max} in Equation 1 that contributes to the 25%, 50% and 75% of the reconstructed data - for the indicative case of the mean flux spectra - in order to identify the source of the differences between $M(i)$ and $M'(i)$ with respect to the re-scaled ECT fluxes. We found that the agreement accounting for the SURF plates $5-8$ was attributed to the re-scaling(s) within the $2-6$ MeV range while the improvement accounting for SREM_S12 and S13 channels was attributed to the adjustments within the $2-3$ MeV. Given these consistent agreements, the change in the median values accounting for $SREM\_C4$ channel - which found to be attributed to adjustments within $3.3 - 4.8$ MeV - can be only justified by the statistically poor resolution of channel's response at this energy range (cf. Figure 3). Figure 5 present - as characteristic examples - the cross-plots between $C_{rec,i}$ and $C'_{rec,i}$ for the case of SURF_7 and SREM_S13 channels.
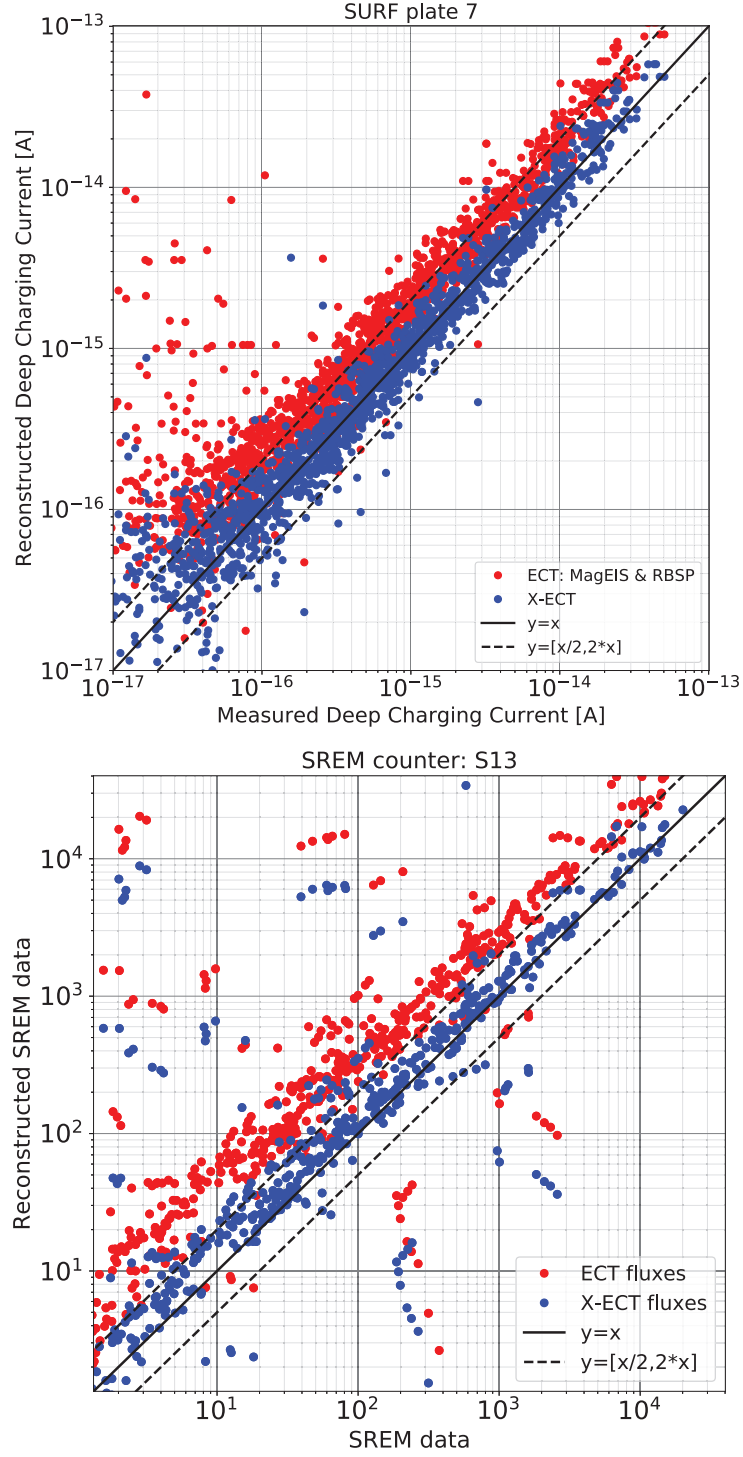
Figure 5. Actual measurements of SURF plate 7 (upper plot) and SREM channel S13 (lower plot) versus reconstructed ones as derived by folding the electron response function with the ECT spectra before (red dots) and after (blue dots) the harmonization of the ECT spectra.

These results validate the harmonization between ECT and XEP relativistic and ultra-relativistic electron flux measurements at least for the energies up to 6.3

Table 2. Summary of validation results using ESA radiation monitor data

Channel	E_{25}, E_{50}, E_{75}	$M(C_{rec}/C)$	$M(C'_{rec}/C)$
SURF_5	1.4, 2.2, 3.4	1.4	1.2
SURF_6	2.6, 3.8, 5.0	2.3	1.3
SURF_7	3.9, 4.8, 5.7	1.9	1.1
SURF_8	5.2, 5.7, 6.2	1.8	1.0
SREM_S12	2.0, 2.3, 2.9	3.7	1.2
SREM_S13	2.1, 2.5, 3.0	3.4	1.2
SREM_C4	3.3, 3.7, 4.8	0.7	0.4

MeV. In addition, they demonstrate the calibration consistency between ESA radiation monitors and XEP.

5 Applications

The harmonization of science-class experiments on board RBSP and ARASE defines an extended reference baseline for the relativistic electron flux measurements from 2012. A reference dataset with the characteristics presented in the previous sections can be used in a series of applications. Space radiation monitors on-board satellites the orbits of which have crossed the HEO of RBSP and Arase can be cross-calibrated under a reference. A typical example to be considered is the case of the MEO radiation measurements from the monitoring units on-board GNSS constellations such as the EU Galileo and the US GPS. In addition, even monitors at GEO can be cross-calibrated as long as they were operating during the Geostationary Transfer Orbit of the carrier satellite. The use of the harmonized relativistic datasets can also contribute to the development or evaluation of quantitative climatological/engineering models based on a large number of different datasets. In such models, like the IRENE (O'Brien et al., 2018), it is important to adopt a reference baseline and use it to identify and eliminate the systematic biases in the considered datasets, and also to quantify their observational uncertainties. Last, a reference megaelectron-volt electron flux dataset with measurements that span almost a decade, can be used for the improvement or the validation of physical or data-driven, e.g. (S. A. Bourdarie & Maget, 2012; Subbotin & Shprits, 2009; Glauert et al., 2014) predictive electron radiation belt models leading to improved forecasts accounting the state of the outer belt.

6 Conclusions

Systematic disagreements in the calibration of trapped energetic electron flux measurements can be crucial for scientific studies based on synergistic observations of energetic electrons and for the outputs of space radiation environment specification models. In this work, we proceeded to the inter-calibration of Arase/XEP and RBSP/ECT measurements. For the harmonization of ultra-relativistic electron fluxes, the criterion of using quiet magnetospheric conditions for the determination of conjunctions was relaxed. The remarkable agreement between XEP and the majority of MagEIS channels was demonstrated, together with the suggestion of adjusting MagEIS/HIGH and REPT measurements accordingly. The harmonization factors for the ECT channels were derived and validated - for at least up to ~ 6 MeV - using measurements from ESA radiation monitors. For $E > 6$ MeV extended investigations will be carried out using GSAT/EMU measurements. The harmonization of corner-stone electron flux measurements defines an extended reference baseline that can be

used in a series of applications; for the calibration of space radiation detectors, for updating/validating quantitative climatological and/or forecasting models addressing the electron radiation environment of the outer Van Allen belt.

References

Agostinelli, S., Allison, J., Amako, K., Apostolakis, J., Araujo, H., Arce, P., . . . Zschiesche, D. (2003, July). Geant4—a simulation toolkit. *Nuclear Instruments and Methods in Physics Research Section A: Accelerators, Spectrometers, Detectors and Associated Equipment*, *506*(3), 250–303. Retrieved from `https://doi.org/10.1016/s0168-9002(03)01368-8` doi: 10.1016/s0168-9002(03)01368-8

Aminalragia-Giamini, S., Sandberg, I., Papadimitriou, C., Daglis, I. A., & Jiggens, P. (2018). The virtual enhancements - solar proton event radiation (VESPER) model. *Journal of Space Weather and Space Climate*, *8*, A06. Retrieved from `https://doi.org/10.1051/swsc/2017040` doi: 10.1051/swsc/2017040

Baker, D. N., Jaynes, A. N., Hoxie, V. C., Thorne, R. M., Foster, J. C., Li, X., . . . Lanzerotti, L. J. (2014, November). An impenetrable barrier to ultra-relativistic electrons in the van allen radiation belts. *Nature*, *515*(7528), 531–534. Retrieved from `https://doi.org/10.1038/nature13956` doi: 10.1038/nature13956

Baker, D. N., Kanekal, S. G., Hoxie, V. C., Batiste, S., Bolton, M., Li, X., . . . Friedel, R. (2012, December). The Relativistic Electron-Proton telescope (REPT) Instrument on Board the Radiation Belt Storm Probes (RBSP) spacecraft: Characterization of earth's radiation belt high-energy particle populations. *Space Science Reviews*, *179*(1-4), 337–381. Retrieved from `https://doi.org/10.1007/s11214-012-9950-9` doi: 10.1007/s11214-012-9950-9

Blake, J. B., Carranza, P. A., Claudepierre, S. G., Clemmons, J. H., Crain, W. R., Dotan, Y., . . . Zakrzewski, M. P. (2013, June). The Magnetic Electron Ion Spectrometer (MagEIS) Instruments Aboard the Radiation Belt Storm Probes (RBSP) Spacecraft. *Space Science Reviews*, *179*(1-4), 383–421. Retrieved from `https://doi.org/10.1007/s11214-013-9991-8` doi: 10.1007/s11214-013-9991-8

Bourdarie, S., Blake, B., Cao, J., Friedel, R., Miyoshi, Y., Panasyuk, M., & Underwood, C. (2008). Data analysis procedure v1.2. *COSPAR*. Retrieved from `http://craterre.onecert.fr/prbem/Data\_analysis.pdf`

Bourdarie, S. A., & Maget, V. F. (2012, June). Electron radiation belt data assim-

ilation with an ensemble kalman filter relying on the salammbô code. *Annales Geophysicae*, *30*(6), 929–943. Retrieved from `https://doi.org/10.5194/angeo-30-929-2012` doi: 10.5194/angeo-30-929-2012

Boyd, A. J., Reeves, G. D., Spence, H. E., Funsten, H. O., Larsen, B. A., Skoug, R. M., . . . Jaynes, A. N. (2019, November). RBSP-ECT combined spin-averaged electron flux data product. *Journal of Geophysical Research: Space Physics*, *124*(11), 9124–9136. Retrieved from `https://doi.org/10.1029/2019ja026733` doi: 10.1029/2019ja026733

Claudepierre, S. G., O'Brien, T. P., Blake, J. B., Fennell, J. F., Roeder, J. L., Clemmons, J. H., . . . Larsen, B. A. (2015, July). A background correction algorithm for Van Allen Probes MagEIS electron flux measurements. *Journal of Geophysical Research: Space Physics*, *120*(7), 5703–5727. Retrieved from `https://doi.org/10.1002/2015ja021171` doi: 10.1002/2015ja021171

Evans, H., Bühler, P., Hajdas, W., Daly, E., Nieminen, P., & Mohammadzadeh, A. (2008). Results from the ESA SREM monitors and comparison with existing radiation belt models. *Advances in Space Research*, *42*(9), 1527 - 1537. Retrieved from `http://www.sciencedirect.com/science/article/pii/S0273117708001737` doi: https://doi.org/10.1016/j.asr.2008.03.022

Glauert, S. A., Horne, R. B., & Meredith, N. P. (2014, January). Three-dimensional electron radiation belt simulations using the BAS radiation belt model with new diffusion models for chorus, plasmaspheric hiss, and lightning-generated whistlers. *Journal of Geophysical Research: Space Physics*, *119*(1), 268–289. Retrieved from `https://doi.org/10.1002/2013ja019281` doi: 10.1002/2013ja019281

Heynderickx, D., Kruglanski, M., Quaghebeur, B., Speelman, E., & Daly, E. J. (2000, July). An overview and discussion of SPENVIS, ESA's space environment information system, and UNILIB, a fortran library of magnetic field utilities. In *SAE technical paper series.* SAE International. Retrieved from `https://doi.org/10.4271/2000-01-2415` doi: 10.4271/2000-01-2415

Heynderickx, D., Sandberg, I., & Jiggens, P. (2018). Solar energetic particle environment modelling reference dataset v2.1. *ESA Technical Note*. Retrieved from `http://sepem.eu/help/SEPEM\_RDS\_v2-01.zip`

Higashio, N., Takashima, T., Shinohara, I., & Matsumoto, H. (2018a, August). The extremely high-energy electron experiment (XEP) onboard the arase (ERG) satellite. *Earth, Planets and Space*, *70*(1). Retrieved from `https://doi.org/10.1186/s40623-018-0901-x` doi: 10.1186/s40623-018-0901-x

Higashio, N., Takashima, T., Shinohara, I., & Matsumoto, H. (2018b, August). The XEP instrument level-2 omniflux data of exploration of energization and radiation in geospace (ERG) arase satellite. , ( ). Retrieved from `https://doi.org/10.34515/DATA.ERG-00001` doi: 10.34515/DATA.ERG-00001

Jaynes, A. N., Baker, D. N., Singer, H. J., Rodriguez, J. V., Loto'aniu, T. M., Ali, A. F., . . . Reeves, G. D. (2015, September). Source and seed populations for relativistic electrons: Their roles in radiation belt changes. *Journal of Geophysical Research: Space Physics*, *120*(9), 7240–7254. Retrieved from `https://doi.org/10.1002/2015ja021234` doi: 10.1002/2015ja021234

Jiggens, P., Heynderickx, D., Sandberg, I., Truscott, P., Raukunen, O., & Vainio, R. (2018). Updated model of the solar energetic proton environment in space. *Journal of Space Weather and Space Climate*, *8*, A31. Retrieved from `https://doi.org/10.1051/swsc/2018010` doi: 10.1051/swsc/2018010

Johnson, M. H., & Kierein, J. (1992, July). Combined release and radiation effects satellite (CRRES): Spacecraft and mission. *Journal of Spacecraft and Rockets*, *29*(4), 556–563. Retrieved from `https://doi.org/10.2514/3.55641` doi: 10.2514/3.55641

Katsavrias, C., Sandberg, I., Li, W., Podladchikova, O., Daglis, I., Papadimitriou, C., . . . Aminalragia-Giamini, S. (2019, June). Highly relativistic electron flux

enhancement during the weak geomagnetic storm of april–may 2017. *Journal of Geophysical Research: Space Physics*, *124*(6), 4402–4413. Retrieved from https://doi.org/10.1029/2019ja026743 doi: 10.1029/2019ja026743

Mann, I. R., Ozeke, L. G., Murphy, K. R., Claudepierre, S. G., Turner, D. L., Baker, D. N., . . . Honary, F. (2016, June). Explaining the dynamics of the ultra-relativistic third van allen radiation belt. *Nature Physics*, *12*(10), 978–983. Retrieved from https://doi.org/10.1038/nphys3799 doi: 10.1038/nphys3799

Mauk, B. H., Fox, N. J., Kanekal, S. G., Kessel, R. L., Sibeck, D. G., & Ukhorskiy, A. (2012). Science objectives and rationale for the Radiation Belt Storm Probes mission. In *The Van Allen Probes mission* (pp. 3–27). Springer US. Retrieved from https://doi.org/10.1007/978-1-4899-7433-4_2 doi: 10.1007/978-1-4899-7433-4_2

Miyoshi, Y., Hori, T., Shoji, M., Teramoto, M., Chang, T. F., Segawa, T., . . . Shinohara, I. (2018b, June). The ERG science center. *Earth, Planets and Space*, *70*(1). Retrieved from https://doi.org/10.1186/s40623-018-0867-8 doi: 10.1186/s40623-018-0867-8

Miyoshi, Y., Shinohara, I., Takashima, T., Asamura, K., Higashio, N., Mitani, T., . . . Seki, K. (2018a, June). Geospace exploration project ERG. *Earth, Planets and Space*, *70*(1). Retrieved from https://doi.org/10.1186/s40623-018-0862-0 doi: 10.1186/s40623-018-0862-0

Mohammadzadeh, A., Evans, H., Nieminen, P., Daly, E., Vuilleumier, P., Buhler, P., . . . Fear, R. (2003). The ESA Standard Radiation Environment Monitor program first results from proba-i and integral. *IEEE Transactions on Nuclear Science*, *50*(6), 2272-2277. doi: 10.1109/TNS.2003.821796

Olson, W. P., & Pfitzer, K. A. (1977). Magnetospheric magnetic field modeling, annual scientific report. *AFOSR Contract No. F44620-75-C-0033*. Retrieved from https://doi.org/10.1109/tns.2019.2915686

Onsager, T., Grubb, R., Kunches, J., Matheson, L., Speich, D., Zwickl, R. W., & Sauer, H. (1996, October). Operational uses of the GOES energetic particle detectors. In E. R. Washwell (Ed.), *GOES-8 and beyond.* SPIE. Retrieved from https://doi.org/10.1117/12.254075 doi: 10.1117/12.254075

O'Brien, T. P., Johnston, W. R., Huston, S. L., Roth, C. J., Guild, T. B., Su, Y. ., & Quinn, R. A. (2018). Changes in AE9/AP9-IRENE version 1.5. *IEEE Transactions on Nuclear Science*, *65*(1), 462-466. doi: 10.1109/TNS.2017.2771324

Reeves, G. D., Friedel, R. H. W., Larsen, B. A., Skoug, R. M., Funsten, H. O., Claudepierre, S. G., . . . Baker, D. N. (2016, January). Energy-dependent dynamics of keV to MeV electrons in the inner zone, outer zone, and slot regions. *Journal of Geophysical Research: Space Physics*, *121*(1), 397–412. Retrieved from https://doi.org/10.1002/2015ja021569 doi: 10.1002/2015ja021569

Richardson, I., Cane, H., von Rosenvinge, T., & McGuire, R. (2008, January). IMP 8 GME Energetic Particle Observations Over Three Solar Cycles. In *International cosmic ray conference* (Vol. 1, p. 323-326).

Ryden, K. A., Hands, A. D. P., Underwood, C. I., & Rodgers, D. J. (2015). Internal charging measurements in medium earth orbit using the surf sensor: 2005–2014. *IEEE Transactions on Plasma Science*, *43*(9), 3014-3020. doi: 10.1109/TPS.2015.2416436

Sandberg, I., Aminalragia-Giamini, S., Provatas, G., Hands, A., Ryden, K., Heynderickx, D., . . . Rodgers, D. (2019, July). Data exploitation of new galileo environmental monitoring units. *IEEE Transactions on Nuclear Science*, *66*(7), 1761–1769. Retrieved from https://doi.org/10.1109/tns.2019.2915686 doi: 10.1109/tns.2019.2915686

Sandberg, I., Jiggens, P., Heynderickx, D., & Daglis, I. A. (2014, July). Cross calibration of NOAA GOES solar proton detectors using corrected NASA IMP-8/GME data. *Geophysical Research Letters*, *41*(13), 4435–4441. Retrieved

from `https://doi.org/10.1002/2014gl060469` doi: 10.1002/2014gl060469

Subbotin, D. A., & Shprits, Y. Y. (2009, October). Three-dimensional modeling of the radiation belts using the versatile electron radiation belt (VERB) code. *Space Weather*, *7*(10), n/a–n/a. Retrieved from `https://doi.org/10.1029/2008sw000452` doi: 10.1029/2008sw000452

Turner, D. L., O'Brien, T. P., Fennell, J. F., Claudepierre, S. G., Blake, J. B., Kilpua, E. K. J., & Hietala, H. (2015, November). The effects of geomagnetic storms on electrons in earth's radiation belts. *Geophysical Research Letters*, *42*(21), 9176–9184. Retrieved from `https://doi.org/10.1002/2015gl064747` doi: 10.1002/2015gl064747

Van Allen, J. A., Baker, D. N., Randall, B. A., & Sentman, D. D. (1974, September). The magnetosphere of jupiter as observed with pioneer 10: 1. instrument and principal findings. *Journal of Geophysical Research*, *79*(25), 3559–3577. Retrieved from `https://doi.org/10.1029/ja079i025p03559` doi: 10.1029/ja079i025p03559